

## Research Article

# Preparation and Photocatalytic Properties of $\text{TiO}_2\text{-Al}_2\text{O}_3$ Composite Loaded Catalysts

Jianzhong Pei,<sup>1</sup> Weisi Ma,<sup>1</sup> Rui Li,<sup>1</sup> Yanwei Li,<sup>2</sup> and Hongzhao Du<sup>3</sup>

<sup>1</sup>School of Highway, Chang'an University, Xi'an, Shaanxi 710064, China

<sup>2</sup>Transport Agency of Shijiazhuang, Shijiazhuang, Hebei 050001, China

<sup>3</sup>Henan Provincial Communications Planning Survey & Design Institute Co., Ltd., Zhengzhou, Henan 450052, China

Correspondence should be addressed to Jianzhong Pei; peijianzhong@126.com

Received 11 August 2014; Revised 30 November 2014; Accepted 21 December 2014

Academic Editor: Kaustubha Mohanty

Copyright © 2015 Jianzhong Pei et al. This is an open access article distributed under the Creative Commons Attribution License, which permits unrestricted use, distribution, and reproduction in any medium, provided the original work is properly cited.

This paper presents an experimental approach to study catalytic effects of  $\text{Fe}^{3+}$  modified nanometer titanium dioxide ( $\text{TiO}_2$ ) loaded on aluminium oxide ( $\text{Al}_2\text{O}_3$ ). Sol-gel method was used to prepare modified  $\text{TiO}_2$  loaded on carrier. Purification tests were conducted in a self-developed instrument to study catalytic effects of  $\text{TiO}_2$  loaded on  $\text{Al}_2\text{O}_3$  with different contents through degradation rate. The modification mechanism was studied by scanning electron microscope (SEM). Results showed that loading on  $\text{Al}_2\text{O}_3$  improved photocatalytic effect of  $\text{TiO}_2$  modified with  $\text{Fe}^{3+}$ . The best photocatalytic effect was achieved under catalytic action of  $\text{Al}_2\text{O}_3$  loaded with 10%  $\text{TiO}_2$  composite; the degradation rates were 6.9%, 13.8%, 21.4%, and 49.2%, respectively, 0.7%, 3.9%, 1.3%, and 15.1% larger than unloaded  $\text{TiO}_2$ . SEM results of four catalysts showed that nanometer  $\text{TiO}_2$  was coated in form of grain on the surface of  $\text{Al}_2\text{O}_3$ . The optimal loading content was 10% at which the nanometer  $\text{TiO}_2$  grains were coated on the surface of  $\text{Al}_2\text{O}_3$  uniformly.

## 1. Introduction

There was a lot of automobile exhaust in the highway tunnels. This exhaust contained a lot of gas phase carbon monoxide (CO), nitrogen oxide ( $\text{NO}_x$ ), hydrocarbons, and other pollutants [1]. Meanwhile, the harmful gas inside tunnels was hard to be expelled, especially in long tunnel encountering long time traffic jams, which would seriously influence driving safety and personnel health [2]. Therefore, it was necessary to reduce harmful gas in tunnels, especially in long tunnel. Semiconductor optical catalyst which emerged in the 1970s was a new oxidation technology, showing good function for degradation of organic pollutants [3].  $\text{TiO}_2$  powders as a kind of photocatalytic materials had been successfully applied in pollutant disposal, especially in sewage treatment and indoor waste gas purification, and certain achievements have been made [4, 5]. However, disadvantages were also shown in actual application. For example, the  $\text{TiO}_2$  was difficult to precipitate and recover due to its tiny particles, during which the active ingredient was lost by a large percentage [6].

In order to solve the problems above, a considerable number of research efforts have been made. At present, photocatalytic materials fixed to a carrier had become a current trend. Nanometer  $\text{TiO}_2$  particle fixed on montmorillonite showed better photocatalytic property, because specific surface area of the nanometer  $\text{TiO}_2$  became bigger when loaded on carriers such as diatom class [7, 8], montmorillonite [9, 10], and kaolinite [11–13], so as to increase utilization rate of the light and absorption ability of pollutants. In addition, a few carriers such as metal chemicals could interact with nanometer  $\text{TiO}_2$  particles, and this interaction was helpful for separation of the electronic hole of nanometer  $\text{TiO}_2$  particles, which could improve the catalytic effect [14]. However, these researches were mainly used for waste water treatment; few studies were conducted in the aspect of gas purification in tunnels. Therefore, the goal of this paper was to (1) research catalytic efficiency of nanometer  $\text{TiO}_2$  loaded on  $\text{Al}_2\text{O}_3$  for major kinds of gases in tail gas and (2) study modification mechanism of the composite materials.

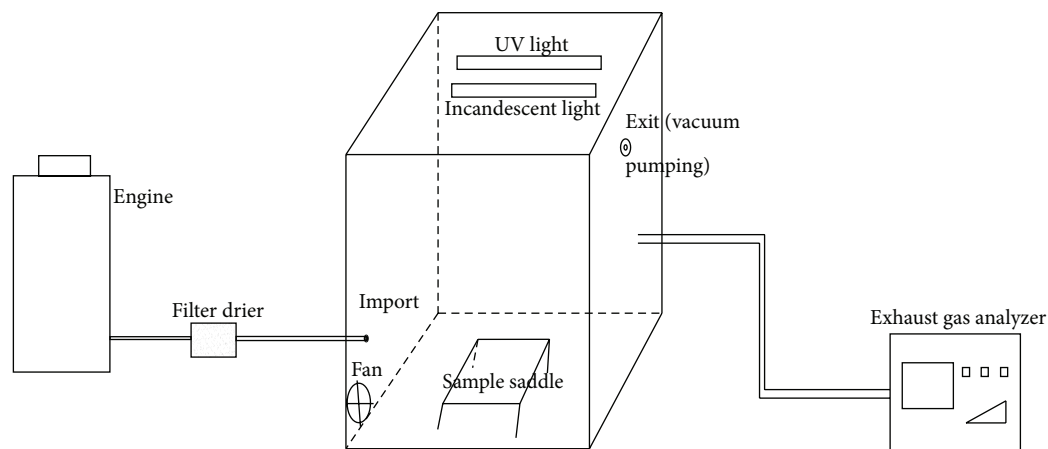


FIGURE 1: Equipment for exhaust gas purification.

## 2. Experimental

**2.1. Preparation of Photocatalytic Materials.** Modified nanometer  $\text{TiO}_2$  was prepared by sol-gel method. (1) Prepare  $\text{TiO}_2$  sol doped with 0.1%  $\text{Fe}^{3+}$ , used as control sample; (2) prepare  $\text{Al}_2\text{O}_3$  saturated solution with a certain amount of alumina and deionized water; (3) the wet gel composed of  $\text{TiO}_2$  sol and  $\text{Al}_2\text{O}_3$  saturated solution was prepared by a 30-minute violent mixing; (4) dry gel was obtained by drying the wet gel in vacuum at  $80^\circ\text{C}$ . (5)  $\text{TiO}_2$  loaded on  $\text{Al}_2\text{O}_3$  was obtained by calcination at  $500^\circ\text{C}$  in a muffle furnace for 2 hours.

Four catalysts were prepared by the above procedures, namely, catalyst 1, catalyst 2, catalyst 3, and catalyst 4, respectively. The details of the catalysts are shown in Table 1.

### 2.2. Test Instruments and Methods

**2.2.1. Test Instruments.** A set of test equipment for exhaust gas purification was developed to conduct purification experiments (see Figure 1). The test equipment was composed of motorcycle engine, filter and reaction tank, and an AVL-4000 exhaust gas analyzer (parameters are shown in Table 2). There were inlet control valves in the lower part of reaction tank, and the exhaust port was wetted in the upper portion of the test equipment. To simulate the natural wind in tunnel, a fan was located in the lower side. Sample bracket for test board coated with photocatalytic materials was located in the bottom. A filter filled with material was installed to prevent dust flowing into the reaction tank. Two kinds of light sources, respectively, ultraviolet (UV) light with a wavelength of 287.5 nm and incandescent light similar to the light in tunnels with a wavelength of 500~700 nm were used in this text.

**2.2.2. Test Method.** Photocatalytic materials produced by sol-gel method were evenly daubed on an organic glass board. The board was 300 mm  $\times$  300 mm in length (shown in Figure 2). The board daubed with photocatalytic materials was put into the homemade exhaust catalytic reaction equipment. Purification tests were conducted under the two kinds



FIGURE 2: Sample board for purification test.

TABLE 1: Four catalysts prepared in this study.

Catalyst type	Notes
Catalyst 1	$\text{TiO}_2$ doped with 0.1% $\text{Fe}^{3+}$ , as the control
Catalyst 2	$\text{Al}_2\text{O}_3$ loaded with 5% catalyst 1
Catalyst 3	$\text{Al}_2\text{O}_3$ loaded with 10% catalyst 1
Catalyst 4	$\text{Al}_2\text{O}_3$ loaded with 15% catalyst 1

TABLE 2: Parameters of AVL-4000.

Gas type	HC (ppm)	CO (%)	$\text{CO}_2$ (%)	$\text{NO}_x$ (ppm)
Testing range	0~20000	0~10	0~20	0~5000
Accuracy	1	0.01	0.1	1

of light sources when the initial concentration was steady. In this text, degradation rate was calculated and used as evaluation index for catalytic property. Concentrations of HC, CO,  $\text{CO}_2$ , and  $\text{NO}_x$  were measured and used to calculate concentration rate with the following equation:

$$\eta = \frac{C_0 - C_1}{C_0} * 100\%, \quad (1)$$

where  $\eta$  was the degradation rate;  $C_0$  was initial concentration;  $C_1$  was concentration in the end of tests.

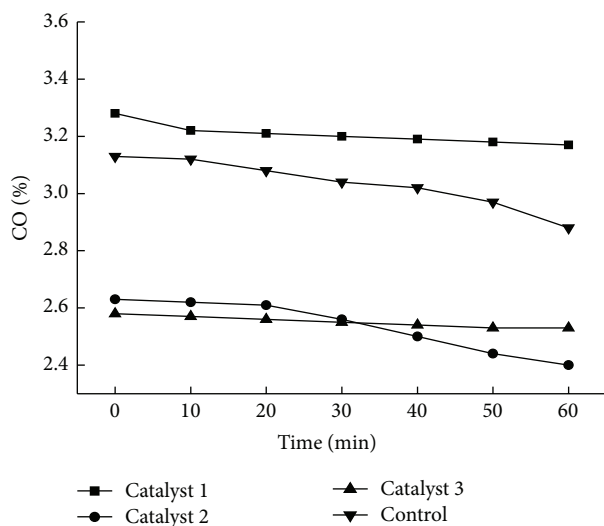


FIGURE 3: Degradation rate of CO under catalytic action of different catalysts.

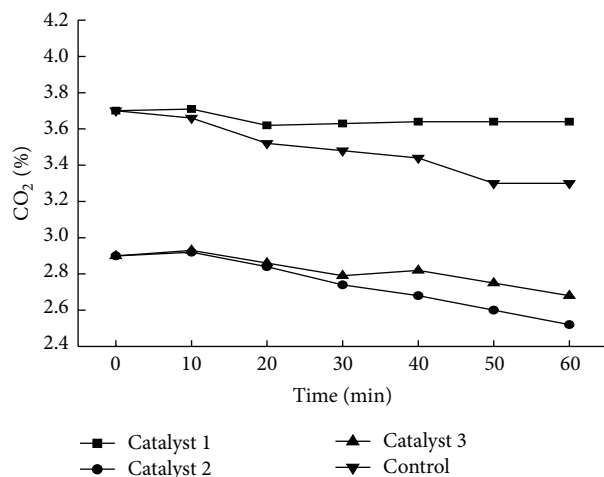


FIGURE 4: Degradation rate of CO<sub>2</sub> under catalytic action of different catalysts.

### 3. Results and Discussion

**3.1. Catalysis of Ultraviolet Light.** The initial concentrations of CO, CO<sub>2</sub>, NO<sub>x</sub>, and HC were recorded after concentration in reaction tank was steady. Test data were measured every 10 min; concentrations of CO, CO<sub>2</sub>, NO<sub>x</sub>, and HC versus time during 60 min were plotted in Figures 3–6. Figures 3–6 represent concentration change of the four gases under catalytic action of unmodified TiO<sub>2</sub> and TiO<sub>2</sub> loaded on Al<sub>2</sub>O<sub>3</sub> with different contents. The differences shown in each figure represent catalytic action of TiO<sub>2</sub> loaded on Al<sub>2</sub>O<sub>3</sub>. It was found that

- (1) change of CO and CO<sub>2</sub> concentration was not apparent, it was mainly because a series of complex REDOX reactions happened under the effect of catalyst between CO and CO<sub>2</sub>, and these reactions were

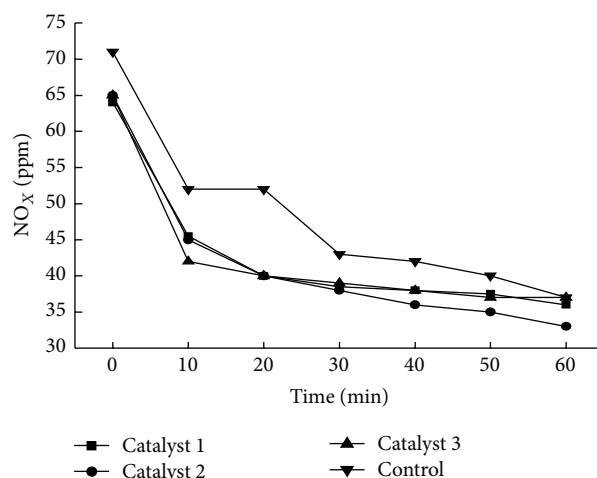


FIGURE 5: Degradation rate of NO<sub>x</sub> under catalytic action of different catalysts.

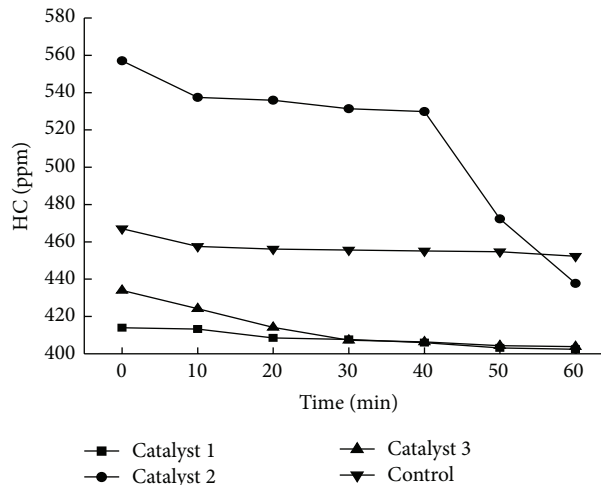


FIGURE 6: Degradation rate of HC under catalytic action of different catalysts.

reversible chemical reactions in which CO and CO<sub>2</sub> acted as reactant and products for each other;

- (2) concentration of HC declined with the increase of action time and it was mainly because HC was decomposed into water and carbon oxide;
- (3) there was notable decline in concentration of NO<sub>x</sub> especially in the first 30 minutes. This is mainly because NO<sub>x</sub> was oxidized into HNO<sub>3</sub> and H<sub>2</sub>O under the action of catalyst.

The quantitative impacts of Fe<sup>3+</sup> on the catalytic effects of TiO<sub>2</sub> are plotted in Figure 7. Degradation rates of four gases were calculated according to data obtained from purification tests and (1). The following findings were observed.

- (1) In general, doping Fe<sup>3+</sup> improved the photocatalysis efficiency of nano-TiO<sub>2</sub>.

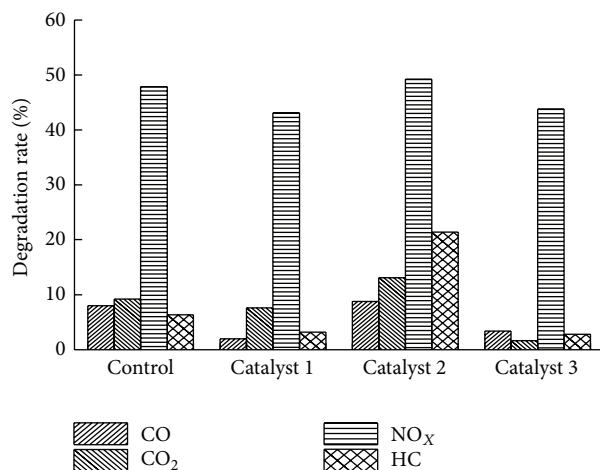


FIGURE 7: Degradation rates of CO, CO<sub>2</sub>, NO<sub>x</sub>, and HC under catalytic action of different catalysts.

- (2) Catalytic effect of catalyst 3 was the best, with degradation rate of CO, CO<sub>2</sub>, HC, and NO<sub>x</sub>, respectively, 6.9%, 13.8%, 21.4%, and 49.2%, increased by 0.7%, 3.9%, 1.3%, and 15.1% compared to TiO<sub>2</sub> unloaded on Al<sub>2</sub>O<sub>3</sub>.
- (3) Compared with the catalysis of catalyst 1, the degradation rates of the four gases under the catalysis of catalyst 2 and catalyst 4 were reduced. Therefore, catalyst loaded on Al<sub>2</sub>O<sub>3</sub> had a significant influence on the catalysis effect. Too high or too low content would reduce the effect of the catalyst. The optimal dose was suggested to be controlled at about 10% in this paper.

**3.2. Catalysis of the Incandescent Light.** The optimal dosage of carrier was obtained at present. Therefore TiO<sub>2</sub> loaded on the optimal dosage of 10% Al<sub>2</sub>O<sub>3</sub> was used to study catalytic effect under natural light in tunnels. To this end, purification experiments were performed under incandescent lamp light, and concentration changes of CO, CO<sub>2</sub>, NO<sub>x</sub>, and HC are, respectively, plotted in Figures 8–11. Each curve in Figure 8 represents concentration change of CO under catalytic action of catalyst 1 and catalyst 3 in natural light condition. It could be found that, under incandescent lamp light condition, concentration of CO, CO<sub>2</sub>, HC, and NO<sub>x</sub> decreased as testing time increased, especially in the action of catalyst 3. Degradation rates of four components of exhaust were, respectively, 1.9%, 2.3%, 5.1%, and 27.8% under the catalytic action of catalyst 3, 0.6%, 0.6%, 2.3%, and 8.2% larger compared to degradation rate under catalyst 1.

To observe quantitatively the impact of Al<sub>2</sub>O<sub>3</sub> on the purification, degradation rates of four components of exhaust were calculated according to (1) and plotted in Figure 12. It could be found that (1) with catalytic action of catalyst 1, compared to catalytic effect under UV light, degradation rates of four gases were decreased by 8.0%, 10.8%, 6.9%, and 20.1%, mainly because the wavelength range of UV is easier to activate TiO<sub>2</sub> and (2) with catalytic action of catalyst 3,

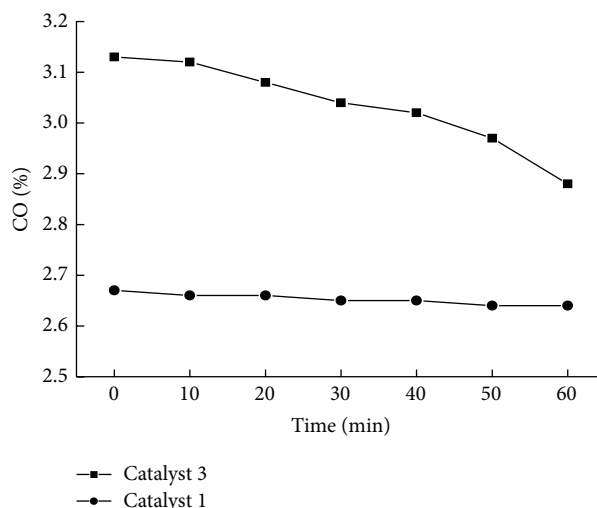


FIGURE 8: Concentration of CO versus time under catalytic effect of catalyst 1 and catalyst 3, respectively.

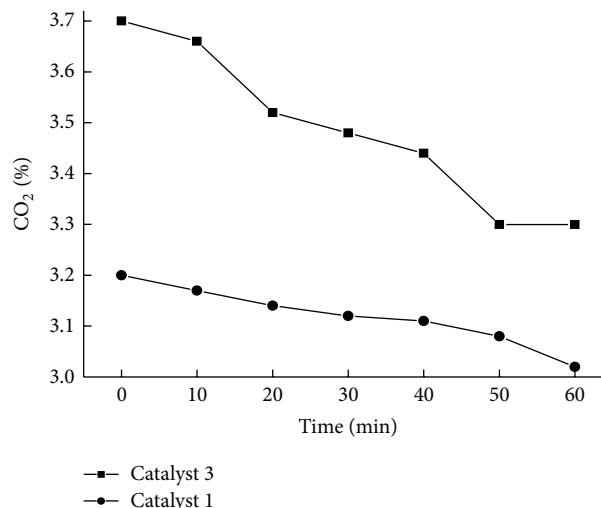


FIGURE 9: Concentration of CO<sub>2</sub> versus time under catalytic effect of catalyst 1 and catalyst 3, respectively.

compared to catalytic effect under UV light, degradation rates of four gases were decreased by 6.1%, 8.5%, 1.8%, and 0%, respectively. It could be concluded that Al<sub>2</sub>O<sub>3</sub> weakened light source sensitivity of TiO<sub>2</sub>.

**3.3. Analysis of Catalytic Process Using GCMS and XRD.** Carrene was used to collect exhaust for 20 minutes. Then the collected exhaust was concentrated by the nitrogen concentration instrument. This first group is the liquor before being catalyzed. As a contrast test, exhaust was collected and then was put in the equipment for exhaust gas purification, and, after 20 minutes, the liquor was taken out and was concentrated by the nitrogen concentration instrument. This second group is the liquor after being catalyzed. Then the first group and second group were tested by GC.

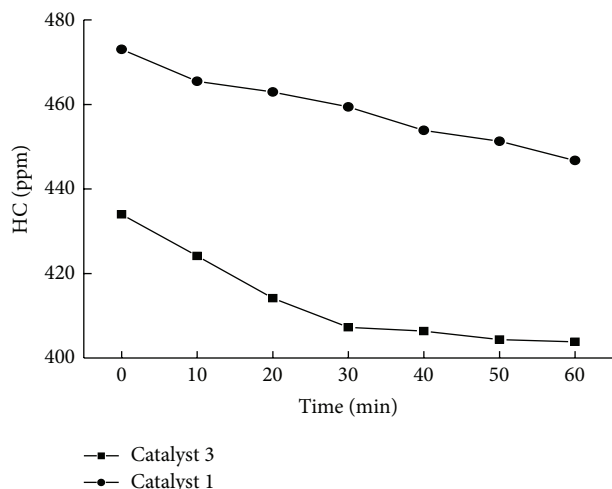


FIGURE 10: Concentration of  $\text{NO}_x$  versus time under catalytic effect of catalysts 1 and 3, respectively.

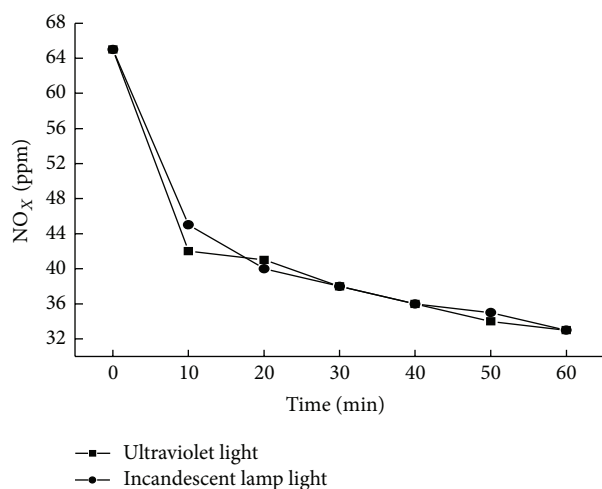


FIGURE 11: Concentration of HC versus time under catalytic effect of catalysts 1 and 3, respectively.

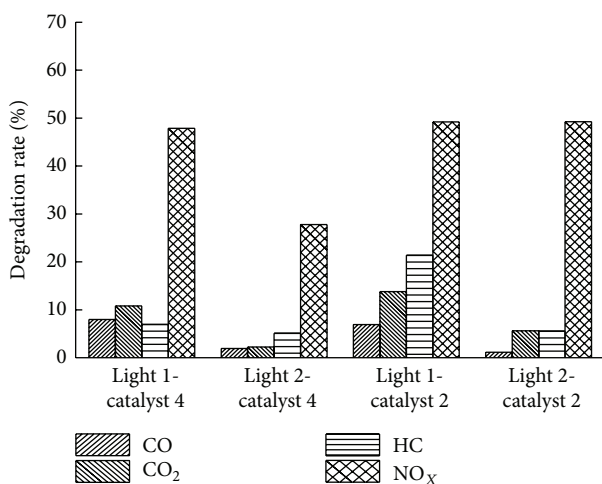


FIGURE 12: Degradation rates of  $\text{CO}$ ,  $\text{CO}_2$ ,  $\text{HC}$ , and  $\text{NO}_x$  under photocatalytic action of catalyst 4 and catalyst 2, UV light and ordinary light condition, respectively.

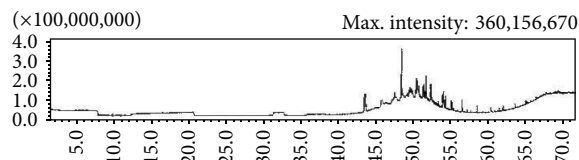


FIGURE 13: Total ionic chromatogram of automobile exhaust.

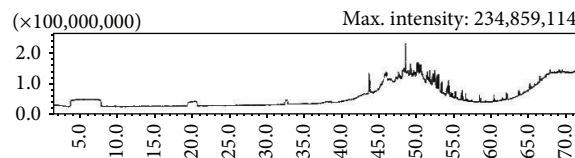


FIGURE 14: Total ionic chromatogram of automobile exhaust after using catalyst.

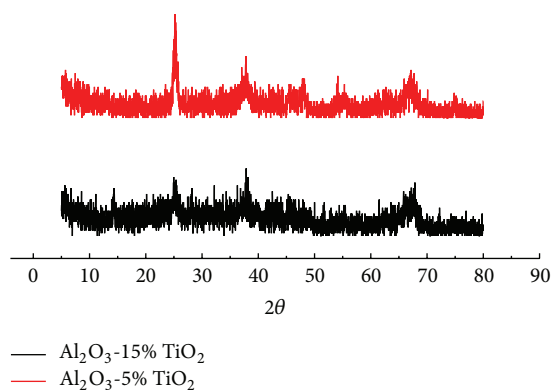


FIGURE 15: XRD of catalysts 2 and 4, respectively.

Total ionic chromatogram of automobile exhaust before and after using catalyst is shown in Figures 13 and 14, respectively. According to Figures 13 and 14, it can be found that most of automobile exhaust concentration has dropped after using catalyst, which can explain that using catalyst can work on reducing automobile exhaust.

X-ray diffraction (XRD) of catalysts 2 and 4 is shown in Figure 15. According to Figure 15, it can be found that XRD of two kinds of catalysts is similar. The diffraction peak intensity and width of two kinds of catalysts are different.  $\text{TiO}_2$  nanoparticles exist on  $\text{Al}_2\text{O}_3$  in the form of particles. Doped  $\text{Al}_2\text{O}_3$  inhibits the growth of  $\text{TiO}_2$  grains. The specific surface area of  $\text{TiO}_2$  nanoparticles increased, so both adsorption capacity and catalytic ability are enhanced. The average particle size of  $\text{TiO}_2$  nanoparticles prepared is 15.2 nm and nano- $\text{TiO}_2$  prepared is anatase phase, so it has higher catalytic efficiency.

**3.4. Analysis of Modification Mechanism.** Photocatalytic reaction rate was closely related to many factors such as catalyst characteristics, system composition, and reactant type. Generally speaking, catalyst features such as  $\text{TiO}_2$  crystal structure and lattice [15],  $\text{TiO}_2$  particle size [16], and electronic defects and hole capture agent had a decisive

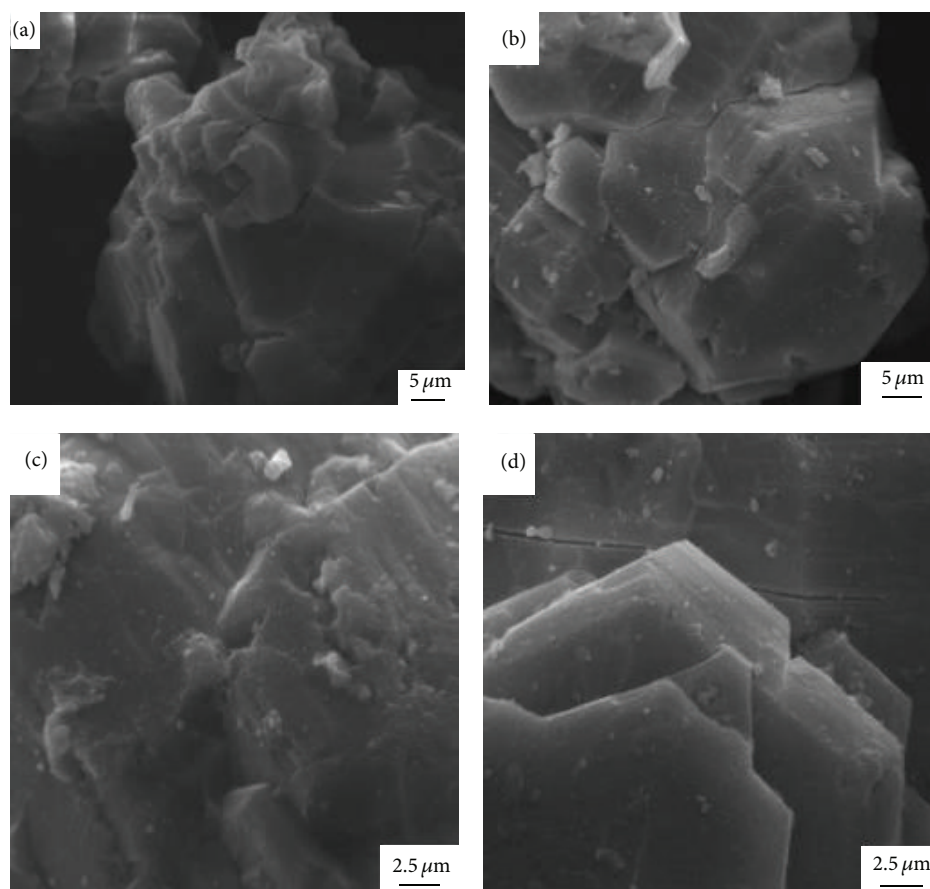


FIGURE 16: The SEM picture of  $\text{TiO}_2$ - $\text{Al}_2\text{O}_3$  composite.

influence on the light-catalyzed role of  $\text{TiO}_2$  [17]. Quanta 200 scanning electron microscope instrument made by FEI was used to make crystal analysis of  $\text{TiO}_2$ - $\text{Al}_2\text{O}_3$  composite, in purpose of analyzing modification mechanism of  $\text{TiO}_2$  composite loaded on  $\text{Al}_2\text{O}_3$ . Parameters of scanning electron microscope instrument were set as follows. Speed up voltage was 20 Kv, and magnification was 10000 times. SEM of modified and unmodified  $\text{TiO}_2$  is plotted in Figure 16.

It could be seen from the scanning electron microscope pictures that there was obvious synergistic reaction between nanometer  $\text{TiO}_2$  and active  $\text{Al}_2\text{O}_3$  grains. Nanometer  $\text{TiO}_2$  were coated in the form of grain with particle size ranging from 10 to 20 nm on the surface of  $\text{Al}_2\text{O}_3$  [18]. Figure 16(a) shows the SEM of  $\text{Al}_2\text{O}_3$  calcining sample; it could be found that surfaces of  $\text{Al}_2\text{O}_3$  were smooth. Figure 16(d) shows the SEM picture of  $\text{Al}_2\text{O}_3$  loaded with 5%  $\text{TiO}_2$ . In this figure, the surfaces of the  $\text{Al}_2\text{O}_3$  were only coated with a handful of  $\text{TiO}_2$  grains, because content of  $\text{TiO}_2$  particles was insufficient to cover the surface of  $\text{Al}_2\text{O}_3$ . Figure 16(c) shows the SEM picture of  $\text{Al}_2\text{O}_3$  loaded with 10%  $\text{TiO}_2$ . In this picture, the  $\text{TiO}_2$  particles were uniformly coated on the surfaces of the  $\text{Al}_2\text{O}_3$  crystals and the  $\text{TiO}_2$  particles kept well hexagonal shapes. These characteristics would accelerate the air pollutants moving to the surfaces of  $\text{TiO}_2$  and make a good contribution to the degradation of the contaminants.

At the same time, the catabolite would leave the  $\text{TiO}_2$  particles quickly. In this way, the catalysis of the  $\text{TiO}_2$  particles was ameliorated. Figure 16(b) showed the magnified patterns of the  $\text{Al}_2\text{O}_3$  loaded with  $\text{TiO}_2$  (15%) calcining sample. It could be seen that  $\text{TiO}_2$  particles were coated on the surface of  $\text{Al}_2\text{O}_3$ . However, the content of  $\text{TiO}_2$  was too large to cause obvious cracks on the surface of  $\text{Al}_2\text{O}_3$ ; photogenerated electrons and holes were covered, resulting in negative influence on the catalysis [19, 20].

#### 4. Conclusions

- (1) Loading on  $\text{Al}_2\text{O}_3$  improved photocatalytic effect of  $\text{TiO}_2$  modified with  $\text{Fe}^{3+}$ , and the best purification effect was achieved when the loaded content of  $\text{TiO}_2$  was 10%. The degradation rates of CO,  $\text{CO}_2$ , HC, and  $\text{NO}_x$  were 6.9%, 13.8%, 21.4%, and 49.2%, respectively, under UV light condition, 0.7%, 3.9%, 1.3%, and 15.1% larger compared to unloaded condition. Under ordinary light condition, degradation rates of the CO,  $\text{CO}_2$ , HC, and  $\text{NO}_x$  were 1.1%, 5.6%, 5.6%, and 49.2%, respectively, almost the same as the results in the ultraviolet light condition.
- (2) It could be seen from the scanning electron microscope pictures that there was obvious synergistic


reaction between nanometer  $\text{TiO}_2$  and active  $\text{Al}_2\text{O}_3$  grains. Nanometer  $\text{TiO}_2$  was coated in form of grain on the surface of  $\text{Al}_2\text{O}_3$ . The optimal loading content was 10%; at this condition, nanometer  $\text{TiO}_2$  grains were coated on the surface of  $\text{Al}_2\text{O}_3$  uniformly.

## Conflict of Interests

The authors declare that there is no conflict of interests regarding the publication of this paper.

## References

- [1] Y. Lei, X. Li, Y. Lu, and H. Xiao, "The advance of the treatment of air pollution in road tunnel," *Techniques and Equipment for Environmental Pollution Control*, vol. 6, no. 2, pp. 40–44, 1998.
- [2] B.-G. Wang, W.-M. Lü, Y. Zhou, M. Shao, and Y.-H. Zhang, "Emission characteristic of PAHs composition in motor vehicles exhaust of city tunnel," *China Environmental Science*, vol. 27, no. 4, pp. 482–487, 2007.
- [3] A. Fujishima and K. Honda, "Electrochemical photolysis of water at a semiconductor electrode," *Nature*, vol. 238, no. 5358, pp. 37–38, 1972.
- [4] W. Shen, W. Zhao, F. He, and Y. Fang, " $\text{TiO}_2$ -based photocatalysis and its applications for waste water treatment," *Progress in Chemistry*, vol. 10, no. 4, pp. 349–361, 1998.
- [5] D. Zhang, R. Qiu, L. Song, B. Eric, Y. Mo, and X. Huang, "Role of oxygen active species in the photocatalytic degradation of phenol using polymer sensitized  $\text{TiO}_2$  under visible light irradiation," *Journal of Hazardous Materials*, vol. 163, no. 2-3, pp. 843–847, 2009.
- [6] W. Haidong, T. Yucui, Z. Hai, and L. I. Hailiang, "Progress in research on  $\text{TiO}_2$ /layer mineral composite," *Materials Review*, vol. 21, no. 6, pp. 134–137, 2001.
- [7] Y.-Y. Su, Y.-Q. Yu, P.-S. Yang, X.-T. Wang, and X.-B. Zhu, "Photocatalytic degradation of anthraquinone dye wastewater with nano- $\text{TiO}_2$ /diatomite," *China Environmental Science*, vol. 29, no. 11, pp. 1171–1176, 2009.
- [8] X. Yu and H. Wei, "Layer-by-layer assembly of  $\text{TiO}_2$  colloids onto diatomite to build hierarchical porous materials," *Advances in Colloid and Interface Science*, vol. 323, pp. 326–331, 2008.
- [9] B. Damardji, H. Khalaf, L. Duclaux, and B. David, "Preparation of  $\text{TiO}_2$ -pillared montmorillonite as photocatalyst Part I. Microwave calcination, characterisation, and adsorption of a textile azo dye," *Applied Clay Science*, vol. 44, no. 3-4, pp. 201–207, 2009.
- [10] F. Li, Y. Jiang, M. Xia, M. Sun, B. Xue, and X. Ren, "A high-stability silica-clay composite: synthesis, characterization and combination with  $\text{TiO}_2$  as a novel photocatalyst for Azo dye," *Journal of Hazardous Materials*, vol. 165, no. 1–3, pp. 1219–1223, 2009.
- [11] M. N. Chong, V. Vimonses, S. Lei, B. Jin, C. Chow, and C. Saint, "Synthesis and characterisation of novel titania impregnated kaolinite nano-photocatalyst," *Microporous and Mesoporous Materials*, vol. 117, no. 1-2, pp. 233–242, 2009.
- [12] Z. Lu, M. Ren, H. Yin et al., "Preparation of nanosized anatase  $\text{TiO}_2$ -coated kaolin composites and their pigmentary properties," *Powder Technology*, vol. 196, no. 2, pp. 122–125, 2009.
- [13] V. Vimonses, M. N. Chong, and B. Jin, "Evaluation of the physical properties and photodegradation ability of titania nanocrystalline impregnated onto modified kaolin," *Microporous and Mesoporous Materials*, vol. 132, no. 1-2, pp. 201–209, 2010.
- [14] L.-R. Lei, Y.-M. Li, and L.-M. Ma, "Pulping effluent treatment with ozone catalyzed by activated carbon and alumina loaded or unloaded with titanium dioxide," *Journal of South China University of Technology (Natural Science)*, vol. 40, no. 2, pp. 149–155, 2012.
- [15] E. Cesca, P. Midrio, R. Boscolo-Berto et al., "Conservative treatment for complex neonatal ovarian cysts: a long-term follow-up analysis," *Journal of Pediatric Surgery*, vol. 48, no. 3, pp. 510–516, 2013.
- [16] S. Montieone, R. Thfeu, A. V. Kanaev, E. Scolan, and C. Sanchez, "Quantum size effect in  $\text{TiO}_2$  nanoparticles: does it exist?" *Applied Surface Science*, vol. 162-163, pp. 565–570, 2000.
- [17] A. V. Emeline, V. Ryabchuk, and N. Serpone, "Factors affecting the efficiency of a photocatalyzed process in aqueous metal-oxide dispersions: prospect of distinguishing between two kinetic models," *Journal of Photochemistry and Photobiology A: Chemistry*, vol. 133, no. 1-2, pp. 89–97, 2000.
- [18] L.-M. Wang, T. Hang, and L.-T. Huang, "Preparation of composite photocatalyst  $\text{TiO}_2$ - $\text{Al}_2\text{O}_3$  and capability of photocatalyst," *Journal of Guizhou University (Natural Science)*, vol. 22, no. 5, pp. 29–31, 2008.
- [19] X. R. Yan, W. W. Guo, K. X. Song, M. L. Huo, and J. P. Wang, "Preparation of nano- $\text{TiO}_2$  film on  $\text{SiO}_2$  and photocatalytic activity," *Acta Energetica Solaris Sinica*, vol. 22, no. 2, pp. 196–199, 2001.
- [20] X.-R. Yan, X.-H. Li, K.-X. Song, H.-T. Zhao, and X.-Z. Chen, "Preparation and characterization of nanometer photocatalysis  $\text{SnO}_2$ @ $\text{TiO}_2$ ," *Chemical Journal of Chinese Universities*, vol. 22, no. 4, pp. 610–613, 2001.



**Hindawi**

Submit your manuscripts at  
<http://www.hindawi.com>

